

Lee-Yang and Langer edge singularities from analytic continuation of scaling functions

Frithjof Karsch¹, Christian Schmidt¹ and Simran Singh¹

¹*Fakultät für Physik, Universität Bielefeld, D-33615 Bielefeld, Germany*

We discuss the analytic continuation of scaling function in the 3-dimensional $Z(2)$, $O(2)$ and $O(4)$ universality classes using the Schofield representation of the magnetic equation of state. We show that a determination of the location of Lee-Yang edge singularities and, in the case of $Z(2)$, also the Langer edge singularity yields stable results. Results for the former are in good agreement with Functional Renormalization Group calculations. We also present results for the location of the Langer edge singularity in the 3- d , $Z(2)$ universality class. We find that in terms of the complex scaling variable z the distance of the Langer edge singularity to the critical point agrees within errors with that of the Lee-Yang edge singularity. Furthermore the magnitude of the discontinuity along the Langer branch cut is an order of magnitude smaller than that along the Lee-Yang branch cut.

January 23, 2024

PACS numbers: 64.10.+h, 75.10.Hk, 05.50+q, 05.10.Cc

I. INTRODUCTION

In the vicinity of a phase transition point the universal critical behavior of thermodynamic observables is parameterized in terms of scaling functions. In studies of the phase structure of the theory of strong-interactions, Quantum Chromodynamics (QCD), scaling functions in the 3- d , $Z(2)$, $O(2)$ and $O(4)$ universality classes play an important role. In particular, when studying QCD at non-zero temperature and with non-vanishing chemical potentials that are the external control parameters for the presence of non-vanishing conserved charge densities, the $O(4)$ universality class controls properties of QCD in the chiral limit while the $Z(2)$ universality class controls the critical behavior in the vicinity of the so-called critical end-point that is expected to exist for large values of the baryon chemical potential [1–3]. When analyzing the phase structure of QCD on discrete space-time lattices parts of the global symmetries are broken explicitly and smaller symmetry groups, e.g. $O(2)$, start playing a role.

In QCD with real, non-vanishing chemical potentials the direct application of numerical methods fails because the integrand of the path integral, defining the QCD partition function, becomes complex. One tries to circumvent this problem by either performing numerical calculations with imaginary chemical potentials [4, 5] or by using Taylor series expansions [6–8], which are set-up at vanishing values of the chemical potential. In both cases it is of importance to understand the analytic structure of the QCD partition function and get control over the location of singularities in the complex plane that hamper analytic continuations on the one hand and limit the radius of convergence of Taylor series on the other hand. This has led to recent interest in the analysis of analytic properties of the universal scaling functions [9, 10] in universality classes that are of relevance for studies of the QCD phase diagram [11–19].

Scaling functions, which describe the singular, universal part of thermodynamic observables, e.g. the order

parameter (M) and its derivatives with respect to temperature T or external field parameter H , are commonly parameterized as function of the real scaling variable $z = z_0 H^{-1/\beta\delta} (T - T_c)/T_c$.

Prominent features of the analytically continued scaling functions in the complex z plane are the occurrence of edge singularities that mark the end-point of branch cuts. In the $Z(2)$ universality class these are the Lee-Yang edge singularity [9, 10] and the so-called Langer edge singularity [20]. In fact, these singularities are expected to be closest to the origin and thus limit the radius of convergence of Taylor series. Both singularities have been discussed extensively [11, 12]. While the phase of the associated cuts in the plane of complex valued scaling variable z is rigorously known to be $\phi_{LY} = \pi/2\beta\delta$ for the Lee-Yang cut and $\phi_{Lan} = \pi(1 - 1/\beta\delta)$ for the Langer cut, the absolute values of the Lee-Yang edge singularity has only been determined recently in Functional Renormalization Group (FRG) calculations [21, 22].

Rather than using (T, H) for the parameterization of thermodynamical observables another set of parameters, (θ, R) , has been introduced by Schofield [23, 24]. This provides a convenient parameterization of the the magnetic equation of state [25, 26], making its dependence on critical exponents explicit. Approximations for the unknown function $h(\theta)$ that enters this parameterization have been determined in analytic as well as numerical calculations [27, 28]. In cases where the analytic form of $h(\theta)$ is exactly known the Schofield parameterization provides straightforwardly an analytic continuation of the scaling functions into the complex z -plane. This is, for instance, the case in the mean-field approximation (MFA) as well as the $N = \infty$ limit of the 3- d , $O(N)$ models. We will discuss this here. The main goal of this work, however, is to examine the analytic continuation of scaling functions using the Schofield parameterization with only approximately known functions $h(\theta)$ as it is currently the case in the $Z(2)$ and $O(N)$ universality classes. We show that a determination of the location of Lee-

Yang edge singularities in these universality classes provides results in good agreement with the FRG analysis [22]. Furthermore, we provide first results for the location of the Langer edge singularity in the analytically continued scaling functions of the 3- d , $Z(2)$ universality class. We also show that the Langer and Lee-Yang cuts can be identified, although details of the expected analytic structure in the vicinity of these edge singularities [9, 10, 12, 20, 29, 30] can not be reproduced when using only a truncated series expansion for the function $h(\theta)$.

This paper is organized as follows. In Sec. II we summarize basic definitions of scaling functions in 3- d universality classes and introduce their representation using the Schofield parameterization of the magnetic equation of state. Sec. III is devoted to a discussion of scaling functions in MFA, the large- N limit of $O(N)$ models, and the $\mathcal{O}(\epsilon^2)$ approximation in the $Z(2)$ universality class, where the generalized linear parametric model (LPM) provides exact results in the Schofield parameterization. In Sec. IV we discuss our results for Lee-Yang edge and Langer edge singularities obtained from the analytic continuation of the Schofield representation of scaling functions. Finally we give an outlook and conclusions in Sec. V. Some details on the determination of the parameterization of scaling functions in the $Z(2)$ universality class are given in Appendix A.

II. SCALING FUNCTIONS IN THE SCHOFIELD PARAMETERIZATION

A. Universal scaling functions

In the vicinity of a critical point the free energy density, $f(T, H)$, of a thermodynamic system contains a non-analytic component, the so-called singular part, $f_f(z)$, which is given in terms of a particular combination of the external control parameters, temperature (T) and symmetry breaking field (H)¹,

$$\frac{f(T, H)}{T} \equiv -\frac{1}{V} \ln Z(T, H) = H_0 h^{1+1/\delta} f_f(z) + \text{reg.} , \quad (1)$$

with

$$z = \frac{t}{h^{1/\beta\delta}} , \quad h \equiv H/H_0 , \quad t = t_0^{-1} \frac{T - T_c}{T_c} . \quad (2)$$

Here the critical temperature T_c as well as the scale parameters H_0 , t_0 are non-universal parameters, whereas the critical exponents β , δ are universal and characteristic for different universality classes. This also is the case for the entire scaling function $f_f(z)$.

In Eq. 1 "reg." denotes additional contributions from regular terms that can be ignored close to the critical point. Thermodynamic observables and their universal scaling behavior can then be described in terms of scaling functions that can be derived from $f_f(z)$. We will consider here the scaling behavior of the order parameter,

$$M = -\frac{\partial f}{\partial H} \equiv h^{1/\delta} f_G(z) , \quad (3)$$

and the magnetic (χ_h) and thermal (χ_t) susceptibilities,

$$\begin{aligned} \chi_h &= \frac{\partial M}{\partial H} = \frac{h^{1/\delta-1}}{H_0} f_\chi(z) , \\ \chi_t &= -T^2 \frac{\partial M}{\partial T} = -\frac{T^2}{t_0 T_c} h^{(\beta-1)/\beta\delta} f'_G(z) . \end{aligned} \quad (4)$$

The scaling functions $f_G(z)$ and $f_\chi(z)$ are related to $f_f(z)$,

$$\begin{aligned} f_G(z) &= -\left(1 + \frac{1}{\delta}\right) f_f(z) + \frac{z}{\beta\delta} f'_f(z) , \\ f_\chi(z) &= \frac{1}{\delta} \left(f_G(z) - \frac{z}{\beta} f'_G(z) \right) . \end{aligned} \quad (5)$$

These scaling functions have been determined in the entire range of real z values using asymptotic expansions for large $|z|$, Taylor series at small z , and Monte Carlo simulations for small and intermediate regions that are either matched to the asymptotic behavior [27, 32, 33] or have been described in terms of the Schofield parameterization of the magnetic equation of state [28, 33]. We will introduce the Schofield parameterization in the following subsection.

B. Schofield parameterization of scaling functions

The scaling functions in the 3- d , $O(N)$ universality classes, including the $Z(2)$ universality class corresponding to $N = 1$, as well as the $N = \infty$ limit, have been determined by using ϵ -expansions and field theoretic methods in 3- d [34–38] as well as numerically using Monte-Carlo simulations [27, 32, 33, 39]. The scaling functions obtained in analytic calculations are commonly parameterized using the Schofield parameterization [23] of the Widom-Griffiths (W-G) [25, 26] form of the magnetic equation of state,

$$M = m_0 R^\beta \theta , \quad (6)$$

$$t = R(1 - \theta^2) , \quad (7)$$

$$h = h_0 R^{\beta\delta} h(\theta) , \quad (8)$$

where (R, θ) denotes an alternative coordinate frame obtained from (t, h) as defined by Eq. 7 and 8 [23, 24].

Using Eqs. 6-8 and comparing these with Eqs. 2 and 3 one easily finds the relation between the scaling functions

¹ We consider here only the leading singular behavior and suppress universal, singular contributions from well-known, corrections-to-scaling (see for instance: [31]).

expressed in terms of z and θ , respectively,

$$f_G(z) \equiv f_G(\theta(z)) = \theta \left(\frac{h(\theta)}{h(1)} \right)^{-1/\delta}, \quad (9)$$

$$z(\theta) = \frac{1 - \theta^2}{\theta_0^2 - 1} \theta_0^{1/\beta} \left(\frac{h(\theta)}{h(1)} \right)^{-1/\beta\delta}. \quad (10)$$

Aside from an explicit dependence on the universal critical exponents, (β, δ) , scaling functions then depend on the function $h(\theta)$, which usually is represented by a polynomial in θ , containing only odd powers of θ . The function $h(\theta)$ is positive in the interval $0 < \theta < \theta_0$, with $\theta_0 > 1$ denoting its first positive real zero. The real z -axis is mapped onto the interval $0 < \theta < \theta_0$. Obviously, $\theta = 1$ corresponds to $z = 0$, $\theta = \theta_0$ corresponds to $z = -\infty$, and $\theta = 0$ corresponds to $z = \infty$.

The prefactors as well as the normalization with $h(1)$, appearing in Eqs. 9 and 10, arise from the scale parameters m_0 and h_0 which can be chosen such that the conventional normalizations for the scaling functions hold; *i.e.* $f_G = 1$ at $z = 0$ and $f_G/(-z)^\beta \rightarrow 1$ for $z \rightarrow -\infty$. This leads to the choice [28],

$$m_0 = \frac{(\theta_0^2 - 1)^\beta}{\theta_0}, \quad h_0 = \frac{m_0^\delta}{h(1)}. \quad (11)$$

The function $h(\theta)$ then provides a parameterization of the magnetic equation of state. Using Eqs. 6-8 and 11 we find

$$M^\delta/h = \theta^\delta \frac{h(1)}{h(\theta)}. \quad (12)$$

Using Eqs. 9 and 10 we also obtain $f'_G(z)$ as,

$$\begin{aligned} f'_G(z) &\equiv \frac{df_G(\theta(z))}{dz} = \frac{df_G}{d\theta} \Big/ \frac{dz}{d\theta} \\ &= -\frac{(\theta_0^2 - 1)(\beta\delta h(\theta) - \beta\theta h'(\theta))}{\theta_0^{1/\beta}(2\beta\delta\theta h(\theta) - (\theta^2 - 1)h'(\theta))} \left(\frac{h(\theta)}{h(1)} \right)^{\frac{1-\beta}{\beta\delta}}. \end{aligned} \quad (13)$$

With this the scaling function of the magnetic susceptibility, defined in Eq. 5, is given by,

$$f_\chi(z) = \frac{((2\beta - 1)\theta^2 + 1)h(1)}{2\beta\delta\theta h(\theta) - (\theta^2 - 1)h'(\theta)} \left(\frac{h(\theta)}{h(1)} \right)^{1-1/\delta}. \quad (14)$$

C. Analytic continuation of the scaling functions

For real values of z the scaling functions $f_\chi(z)$ and $f'_G(z)$ are finite and vanish in the limit $z \rightarrow \pm\infty$. In the Schofield parameterization they thus vanish at $\theta = 0$ and $\theta = \theta_0$. For complex values of θ they, however, develop singularities, which are end-points of cuts in the complex plane. The locations of these edge singularities are obtained as solutions of

$$\begin{aligned} 0 &= \frac{dz(\theta)}{d\theta} \\ \Leftrightarrow 0 &= 2\beta\delta\theta h(\theta) - (\theta^2 - 1)h'(\theta) \end{aligned} \quad (15)$$

Well-known singularities in the complex z -plane refer to the Lee-Yang edge singularities [9, 10] and the Langer edge singularity [20, 40],

$$z_{LY} = |z_{LY}|e^{i\phi_{LY}}, \quad \phi_{LY} = \pi/2\beta\delta, \quad (16)$$

$$z_{Lan} = |z_{Lan}|e^{i\phi_{Lan}}, \quad \phi_{Lan} = \pi(1 - 1/\beta\delta), \quad (17)$$

where the phases ϕ_{LY} and ϕ_{Lan} give the orientation of cuts in the complex z -plane.

We want to extract here information on the location of these singularities using an analytic continuation of the Schofield parameterization with input for the functions $h(\theta)$ that has been obtained for different universality classes and real values of θ . As the mapping $z \Leftrightarrow \theta$ is in general not unique, we will determine the region in the complex θ -plane that provides a unique mapping between z and θ and is connected to the real interval $0 \leq \theta \leq \theta_0$ onto which the real z -axis is mapped. We do so by following lines of complex z values with constant phase,

$$z(\theta) \equiv |z|e^{i\phi}, \quad -\pi \leq \phi < \pi. \quad (18)$$

All these lines start at $\theta = 1$, which corresponds to $|z| = 0$, and will end in points θ_n that correspond to zeroes of the function $h(\theta)$. In particular, we note that $h(\theta)$ may change sign at θ_0 and become negative for real θ in an interval $\theta_0 < \theta < \theta_1$, with θ_1 denoting a possibly existing second real zero of the function $h(\theta)$. In this interval one finds from Eq. 10 that z becomes complex with a phase $\text{Arg}(z) = \pm\pi(1 - 1/\beta\delta)$. On the other hand, points on the imaginary θ -axis correspond to complex z values with phase $\text{Arg}(z) = \pm\pi/2\beta\delta$. Certain θ -intervals on the real and imaginary θ -axis thus have phases corresponding to those of the Langer and Lee-Yang cuts, respectively. However, we note that Eq. 18 implies that also in the complex θ -plane lines exist on which the corresponding z -values have these phase values. We will discuss implications for the location of edge singularities in the complex θ -plane in the following sections.

III. ANALYTIC CONTINUATION OF THE (GENERALIZED) LINEAR PARAMETRIC MODEL

Approximations for the function $h(\theta)$, which is an odd function of θ [12], have been derived as polynomials in θ [34, 38]. To order θ^3 this function depends on a single parameter (θ_0), which gives the only non-trivial zero of $h(\theta)$. Having $\theta_0 > 1$ ensures that the real z -axis can be mapped onto the interval $0 \leq \theta \leq \theta_0$. This is the so-called linear parametric model (LPM) [23]. We generalize this ansatz here to allow θ_0 to be a g -fold zero. In the following we will discuss the two cases,

$$h(\theta) = \theta(1 - (\theta/\theta_0)^2)^g, \quad g = 1, 2, \quad (19)$$

which arise as exact results for the function $h(\theta)$ in mean-field calculations ($g = 1$) and in the $N = \infty$ limit of

3- d , $O(N)$ models ($g = 2$). Moreover, the LPM ansatz with ($g = 1$) also gives the exact result for $h(\theta)$ in the 3- d , $Z(2)$ universality class when calculated to $\mathcal{O}(\epsilon^2)$ in a systematic ϵ -expansion [41, 42]. We will discuss these cases in the following two subsections.

A. Mean field approximation and large- N limit of $O(N)$ models

In MFA as well as in the ($N = \infty$) limit of models in the 3- d , $O(N)$ universality class the scaling function $f_G(z)$ obeys a simple relation [43],

$$f_G(z + f_G^2)^g = 1, \quad (20)$$

with $g = 1$ in mean-field models and $g = 2$ in the ($N = \infty$) limit. This equation can easily be solved for $g = 1$,

$$f_G(z) = \frac{2^{1/3} (9 + \sqrt{12z^3 + 81})^{2/3} - 2 \cdot 3^{1/3} z}{6^{2/3} (9 + \sqrt{12z^3 + 81})^{1/3}}, \quad (21)$$

from which one derives the related susceptibility scaling functions $f'_G(z)$ and $f_\chi(z)$ introduced in Eqs. 13 and 14. This, however, is not at all straightforward to be done for $g = 2$. In that case the LPM approximation of the magnetic equation of state provides an easy to handle parameterization of $f_G(z)$.

Making use of Eq. 20 and critical exponents in the mean-field and ($N = \infty$) universality classes,

$$\beta = \frac{1}{2}, \quad \delta = \begin{cases} 3, & \text{mean-field} \\ 5, & N = \infty \end{cases}, \quad (22)$$

one can determine the function $h(\theta)$ entering the Schofield parameterization of the scaling function $f_G(\theta(z))$. We solve Eq. 9 for $h(\theta)$ and insert this in Eq.10. Inserting this result for $z(\theta, f_G)$ in Eq. 20 yields

$$f_G = \left(\left(\frac{\theta_0}{\theta} \right)^2 \frac{1}{\theta_0^2 - 1} \left(1 - \left(\frac{\theta}{\theta_0} \right)^2 \right) \right)^{-g/\delta}. \quad (23)$$

Here we kept g and δ for clarity. However, in deriving Eq. 23 we already made use of the relation $\delta = 1 + 2g$. Inserting this result for f_G on the left side of Eq. 9 we can solve for $h(\theta)/h(1)$,

$$\frac{h(\theta)}{h(1)} = \theta \left(\frac{\theta_0^2}{\theta_0^2 - 1} \right)^g \left(1 - \left(\frac{\theta}{\theta_0} \right)^2 \right)^g, \quad (24)$$

or equivalently,

$$h(\theta) = \theta \left(1 - \left(\frac{\theta}{\theta_0} \right)^2 \right)^g. \quad (25)$$

This is the linear parametric model for the parameterization of the magnetic equation of state in the MFA ($g = 1$)

and its generalization to the $N \rightarrow \infty$ limit ($g = 2$). We may use this form of $h(\theta)$ to analyze the analytic structure of scaling functions in MFA and the large- N limit, using the Schofield parameterization. In particular, we can determine the location of Lee-Yang edge singularities.

1. Lee-Yang edge singularities

Inserting in Eq. 15 $h(\theta)$ taken from Eq. 25 allows to determine the location of singularities in the scaling functions in the complex θ -plane. For the generalized LPM this gives,

$$0 = \theta_0^2 - (-2\beta\delta\theta_0^2 + 2g + \theta_0^2 + 1)\theta^2 + (-2\beta\delta + 2g + 1)\theta^4. \quad (26)$$

In the case of the MFA and in the large- N limit this quartic equation in θ reduces to a quadratic equation, and one thus obtains only one pair of singularities located at

$$\tilde{\theta}_\pm = \pm \frac{\theta_0}{\sqrt{\delta - (\delta - 1)\theta_0^2}}. \quad (27)$$

Obviously, in the complex θ -plane the location of singularities in the susceptibilities depends on the value of θ_0 . In particular, the singular points are shifted to infinity for

$$\theta_{0,\infty}^2 = \frac{\delta}{\delta - 1}, \quad (28)$$

while they are real for $\theta_0 < \theta_{0,\infty}$ and purely imaginary for $\theta_0 > \theta_{0,\infty}$. Nonetheless, one easily verifies that

$$z(\theta) = \frac{(1 - \theta^2)\theta_0^2}{\theta_0^2 - 1} \left(\frac{\theta_0^2 - \theta^2}{\theta_0^2 - 1} \right)^{-(\delta-1)/\delta} \theta^{-2/\delta} \quad (29)$$

is independent of θ_0 for $\theta = \tilde{\theta}_\pm$. Using $\tilde{\theta}_\pm$ one finds the universal location of the Lee-Yang edge singularity in the complex z -plane,

$$\begin{aligned} z_{LY} \equiv z(\tilde{\theta}_\pm) &= \frac{\delta}{\delta - 1} (1 - \delta)^{1/\delta} \\ &= \begin{cases} 3 \cdot 2^{-2/3} e^{\pm i\pi/3}, & \text{mean-field} \\ 5 \cdot 2^{-8/5} e^{\pm i\pi/5}, & N = \infty \end{cases} \end{aligned} \quad (30)$$

We note that in MFA as well as in the large- N limit the mapping $z \leftrightarrow \theta$ is unique for all z and maps the complex z -plane to the complex θ half-plane with $Re(\theta) \geq 0$. For the specific choice $\theta_0 \equiv \pm\theta_{0,\infty}$ we show this mapping for both cases in Fig. 1. The lines $z = |z| \exp(\pm i\pi/2\beta\delta)$ approach the Lee-Yang edge singularity at $|\theta| = \infty$ and then bifurcate. In both cases the two branches then approach one of the two points at which $h(\theta)$ vanishes, *i.e.* they either approach $\theta = 0$ or θ_0 . These points get approached by the two branch cut lines in the complex z -plane that correspond either to the imaginary or real axis of the θ -plane.

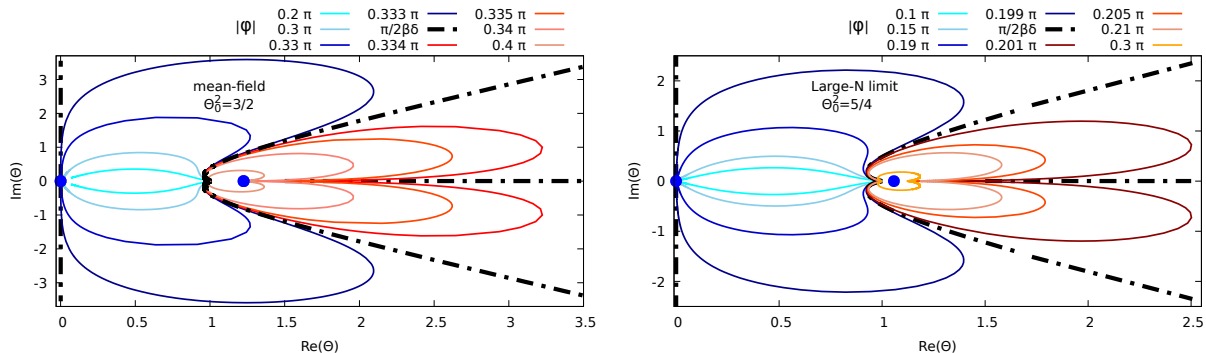


Figure 1. Mapping of the complex z -plane to the complex θ -plane. Shown are lines of z with constant phase ϕ as introduced in Eq. 18, $z = |z|e^{i\phi}$. The left hand figure is for the MFA and the right hand side shows results for the $N = \infty$ limit. Dash-dotted lines correspond to z -values having phase $\phi = \pi/2\beta\delta = \pi/\delta$. Blue dots show points at which $h(\theta) = 0$.

B. LPM for scaling functions in the 3-d, $Z(2)$ universality class

Scaling functions in the 3-d, $Z(2)$ universality class have been determined using analytic as well as numerical approaches. In particular, using the ϵ -expansion, it has been pointed out that to $\mathcal{O}(\epsilon^2)$ the LPM approximation for the function $h(\theta)$ remains exact [41, 42]. One thus obtains $h(\theta)$ as given in Eq. 25 with $g = 1$ and

$$\theta_0^2 = \frac{3}{2}(1 - \epsilon^2/12) + \mathcal{O}(\epsilon^3). \quad (31)$$

New features arise from the fact the product of critical exponents, $\beta\delta$ now deviates from $3/2$. The coefficient of the $\mathcal{O}(\theta^4)$ term, appearing in Eq. 26, thus no longer vanishes.

Using also results for the critical exponents to $\mathcal{O}(\epsilon^2)$,

$$\beta = \frac{1}{2} - \frac{1}{6}\epsilon + \frac{1}{162}\epsilon^2 + \mathcal{O}(\epsilon^3), \quad (32)$$

$$\delta = 3 + \epsilon + \frac{25}{54}\epsilon^2 + \mathcal{O}(\epsilon^3), \quad (32)$$

$$\beta\delta = \frac{3}{2} + \frac{1}{12}\epsilon^2 + \mathcal{O}(\epsilon^3), \quad (33)$$

we may again determine the location of singularities of the susceptibilities using Eq. 26. We now obtain two pairs of solutions for the location of singular points in the complex θ plane,

$$\tilde{\theta}_{p,m}^2 = \frac{A \pm \sqrt{A^2 - 4B\theta_0^2}}{2B}, \quad (34)$$

with

$$A = 1 + 2g + \theta_0^2 - 2\beta\delta\theta_0^2, \quad (35)$$

$$B = 1 + 2g - 2\beta\delta.$$

Obviously, in the 3-d, $Z(2)$ universality class² ($g = 1$)

and with the critical exponents given in Table I, one has $B < 0$.

The square root appearing in Eq. 34 thus is positive and larger than $|A|$. Therefore, irrespective of the value of θ_0 one always finds that $\tilde{\theta}_p^2$ and $\tilde{\theta}_m^2$ are real, but have opposite sign. This gives rise to a pair of real as well as a pair of purely imaginary roots,

$$\theta_{Lan,\pm} \equiv \pm\sqrt{\tilde{\theta}_p^2} = \pm\sqrt{\frac{A + \sqrt{A^2 - 4B\theta_0^2}}{2B}},$$

$$\theta_{LY,\pm} \equiv \pm\sqrt{\tilde{\theta}_m^2} = \pm\sqrt{\frac{A - \sqrt{A^2 - 4B\theta_0^2}}{2B}}. \quad (36)$$

Using the $\mathcal{O}(\epsilon^2)$ results for θ_0 and the critical exponents β , δ one finds for the location of these singular points in the θ -plane³

$$\theta_{Lan,+} = 2.03038,$$

$$\theta_{LY,\pm} = \pm 3.31198 i. \quad (37)$$

As discussed above singular points in the z -plane, corresponding to purely real or imaginary θ values, have phases $\pi(1 - 1/\beta\delta)$ and $\pi/(2\beta\delta)$, respectively. These are the expected phases of cuts emerging from the Langer and Lee-Yang edge singularities.

We get for the singular points

$$z_{Lan} = 2.24047 e^{i\pi(1-1/\beta\delta)},$$

$$z_{LY,\pm} = 2.30674 e^{\pm i\pi/2\beta\delta}. \quad (38)$$

The corresponding mapping of the complex z -plane to the θ -plane is shown in Fig. 2. As can be seen, just like in the MFA, the complex z -plane is mapped onto the entire complex θ half-plane with $\text{Re}(\theta) \geq 0$. We will discuss in the next section that this becomes quite different when using approximations for $h(\theta)$ that go beyond the LPM approximation.

² For the $O(N)$, $N > 1$ universality classes one finds $B > 0$ when $g = 2$.

³ Note that $\theta_{Lan,-}$ lies outside the region used for the unique mapping $z \leftrightarrow \theta$.

	M-F	$\mathcal{O}(\epsilon^2)$, $Z(2)$	$Z(2)$	$O(2)$	$O(4)$	$O(\infty)$
β	1/2	0.3395	0.32643(7)	0.34864(7)	0.380(2)	1/2
δ	3	4.4630	4.78982(85)	4.7798(5)	4.824(9)	5
$\beta\delta$	1.5	1.5833	1.56354(8)	1.6664(5)	1.833(13)	2.5

Table I. Critical exponents in the 3- d , $Z(2)$, $O(2)$ and $O(4)$ universality classes. $Z(2)$ critical exponents are taken from [44, 45] and the $O(2)$ values are taken from [46]. Exponents used for the $O(4)$ case are taken from [47]. Also shown are results obtained in 3- d mean-field theory, results from $\mathcal{O}(\epsilon^2)$ expansion for the 3- d , $Z(2)$ theory, and the $N = \infty$ limit.

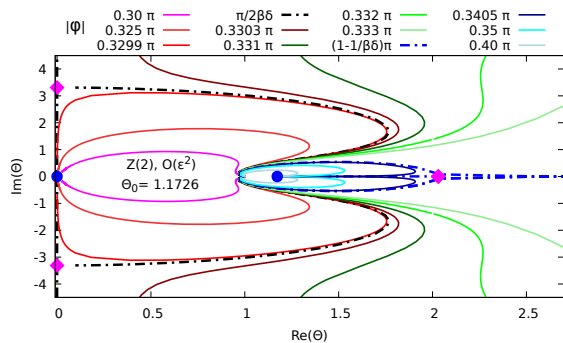


Figure 2. Contours in the complex θ -plane defined by a fixed phase of z , $z = |z| \exp(i\phi)$ obtained by using parameters calculated in an ϵ -expansion to $\mathcal{O}(\epsilon^2)$ [34, 42]. The dash-dotted black lines corresponds to z -values with phase $\phi = \pm\pi/2\beta\delta$, as expected for a Lee-Yang edge singularity and the dash-dotted blue line corresponds to a cut with phase as expected for the Langer cut, $\phi = \pi(1 - 1/\beta\delta)$. Blue dots correspond to points at which $h(\theta) = 0$ and magenta diamonds correspond to $z'(\theta) = 0$.

IV. BEYOND THE LPM APPROXIMATION

We now consider the Schofield parameterization for scaling functions in the $Z(2)$ and $O(N)$ universality classes making use of the known critical exponents in these universality classes (see Table I) and all parameters that have currently been determined for the approximation of the function $h(\theta)$. We parameterize corrections to the generalized LPM approximation as an even polynomial in θ [36]

$$h(\theta) = \theta \left(1 - \left(\frac{\theta}{\theta_0} \right)^2 \right)^g (1 + c_2\theta^2 + c_4\theta^4 + \mathcal{O}(\theta^6)) , \quad (39)$$

with $g = 1, 2$ for the $Z(2)$ and $O(N)$ universality classes, respectively.

In the case of the $Z(2)$ universality class we will also use the commonly used polynomial representation, where the first non-trivial real zero of $h(\theta)$ is not factored out explicitly, *i.e.* we use [34, 48]

$$h(\theta) = \theta (1 + h_3\theta^2 + h_5\theta^4 + h_7\theta^6 + \mathcal{O}(\theta^8)) . \quad (40)$$

Obviously the parameters $(\theta_0, c_2, c_4, \dots)$ can be expressed in terms of (h_3, h_5, h_7, \dots) . In particular, to this order one has $h_7 = -c_4/\theta_0^2$. We give further details on the relation between (h_3, h_5, h_7) and (θ_0, c_2, c_4) in Appendix A.

In the $Z(2)$ universality class the coefficients h_3 , h_5 and h_7 have been calculated [34, 35]. However, usually only the coefficients h_3 and h_5 , corresponding to non-vanishing θ_0 and c_2 , are quoted as the coefficients h_7 , c_4 are small and vanish within current errors. For the case of the $O(N)$ universality class ($N = 2, 4$) a first determination of c_4 , based on fits to Monte Carlo simulation data for $O(2)$ and $O(4)$ scaling functions [39], has been presented recently [28] and also results, based on a 3- d , perturbative calculation have been obtained for the $O(2)$ universality class [37]. We note that results obtained for θ_0 and c_2 obtained in this calculation are in good agreement with the Monte Carlo results when setting $c_4 = 0$. However, values for c_4 obtained in the analytic calculations differ in sign from the current Monte Carlo results. Like in the $Z(2)$ case we thus expect that current results on c_4 still have large uncertainties.

In order to be able to discuss the influence of a non-vanishing next to leading order correction ($c_4 \neq 0$) on the structure of the Schofield parameterization of scaling functions we also calculated c_4 for the $Z(2)$ case using results obtained already in [34, 35]. Although c_4 vanishes within errors, including it in our analysis allows to discuss the influence of such a correction on the determination of singularities of scaling functions in the complex z -plane. Some details on the calculation of h_7 and as such c_4 are given⁴ in Appendix A. This results in the expansion coefficients (h_3, h_5, h_7) in the $Z(2)$ universality class,

$$\begin{aligned} h_3 &= -0.7595(18) , \quad h_5 = 0.00813(68) , \\ h_7 &= 0.00045(127) . \end{aligned} \quad (41)$$

Here we also made use of recent updates on critical exponents in the $Z(2)$ universality class [44, 45]. The effect mainly is to reduce errors on h_3 and h_5 . The parameter sets (θ_0, c_2, c_4) , used in our calculations for the determination of edge singularities in the $Z(2)$, $O(2)$ and $O(4)$ universality classes, are given in Table II.

Aside from the zero θ_0 , which is factored out explicitly in the representation of $h(\theta)$ given in Eq. 39, the additional polynomial factor up to $\mathcal{O}(\theta^4)$ gives rise to two

⁴ This also allows to correct the expression given for h_7 in [34], where a sign factor for one of the terms contributing to h_7 does not show up.

	$Z(2)$ [35]	$O(2)$ [28]	$O(4)$ [28]
θ_0	1.1564(40)	1.610(14)	1.359(10)
c_2	-0.0117(33)	0.162(20)	0.306(34)
c_4	-0.0006(17)	-0.0226(18)	-0.00338(25)
θ_1	9.2(1.3)	1.993(86) i	1.777(106) i
θ_2	$-\dagger$	3.34(21)	9.68(92)

Table II. Parameters entering the definition of $h(\theta)$ in the 3- d , $Z(2)$, $O(2)$ and $O(4)$ universality classes. $Z(2)$ values are taken from [35] and the $O(2)$ and $O(4)$ values are taken from [28].

[†]For $Z(2)$ we only quote a result for the second zero of $h(\theta)$ obtained with $c_4 = 0$ as h_7 and as such c_4 vanish within errors.

additional zeroes in terms of θ^2 ,

$$h(\theta) = \theta \left(1 - \left(\frac{\theta}{\theta_0} \right)^2 \right)^g \left(1 - \left(\frac{\theta}{\theta_1} \right)^2 \right) \left(1 - \left(\frac{\theta}{\theta_2} \right)^2 \right). \quad (42)$$

Results for the zeroes, θ_1 and θ_2 , are also given in Table II.

The main difference in the singular structure of the $Z(2)$ and $O(N)$ scaling functions in the complex z -plane arises from the first correction to the generalized LPM approximation, *i.e.* from c_2 being non-zero and having different signs in both cases. In the $Z(2)$ universality class $c_2 < 0$, while $c_2 > 0$ in the $O(N)$ universality classes. For $c_4 = 0$ it is straightforward to see that as a consequence the new zero, θ_1 , is real in the case of $Z(2)$ and imaginary for the $O(N)$ cases. This in turn results in the presence of the Langer cut [20] in the $Z(2)$ universality class and its absence in the $O(N)$ universality classes:

As discussed in Sec.II, points at which susceptibility scaling functions become singular, are obtained as zeroes of $z'(\theta)$. The condition $z'(\theta) = 0$ led to Eq. 15, which we may rewrite as

$$z'(\theta) = 0 \Leftrightarrow \frac{h'(\theta)}{h(\theta)} = 2\beta\delta \frac{\theta}{\theta^2 - 1}. \quad (43)$$

This relation makes it clear that

- a singularity in the scaling functions exists in the interval $0 < |\theta| < |\theta_1|$ on the imaginary θ -axis, if $h(\theta)$ has a zero, θ_1 , on the imaginary θ -axis,
- a singularity in the scaling functions is located on the real θ -axis, if $h(\theta)$ has a second real zero, $\theta_1 > \theta_0 > 1$, on the real axis.

In the $Z(2)$ case $h_5 > 0$ and it follows from Eq. A11 that $c_2 < 0$ as c_4 is at least an order of magnitude smaller and vanishes within errors. One thus finds a singularity on the real θ -axis. This singularity is located at a complex valued $z \equiv z_{Lan}$ with a phase $\phi_{Lan} = \pi(1 - 1/\beta\delta)$. It is the Langer edge singularity.

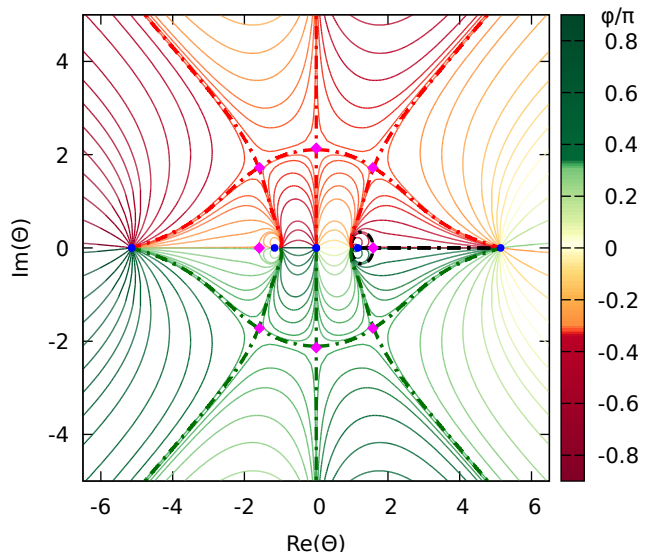


Figure 3. Contours in the entire complex θ -plane. Shown are lines $z = |z|e^{i\phi}$ with constant phase $\phi \in [-\pi, \pi]$. Blue dots correspond to points at which $h(\theta) = 0$ and magenta diamonds correspond to $z'(\theta) = 0$. The dash-dotted lines correspond to the cases $\phi = \phi_{Lan}$ (black) and $\phi = \pm\phi_{LY}$ (red/green), respectively.

In the $O(N)$ cases $c_2 > 0$. Consequently one finds a singularity on the imaginary θ -axis. Actually, it is present for all $c_4 \leq 0$. This singularity is located at a complex valued $z \equiv z_{LY,b}$, with a phase $\phi_{LY} = \pi/2\beta\delta$, which is the phase expected for a Lee-Yang edge singularity. Apparently this singularity in the $O(N)$ universality class is the counter part to the Langer edge singularity in the $Z(2)$ universality class. It is located on the Lee-Yang cut, but it is not located at its edge. The Lee-Yang edge singularity arises from the second pair of singular points that is present for $c_2 \neq 0$ and lies in the complex θ - or z -plane, respectively. This is the case in the $Z(2)$ as well as the $O(N)$ universality classes. The phase of z corresponding to this singular point is not immediately apparent from the general structure of $h(\theta)$. However, we show in the following that, within the current statistical and truncation errors in the approximation for $h(\theta)$, the phase of z is indeed consistent with ϕ_{LY} . These singular points in the complex valued θ -plane with non-zero real and imaginary parts of θ_{LY} define the Lee-Yang edge singularities at $z \equiv z_{LY}$. We present their determination in the $Z(2)$ and $O(N)$ universality classes separately in the following two subsections.

A. Lee-Yang edge singularities in the $Z(2)$ universality class

Using the parameterization of $h(\theta)$ given in Eq. 40 we determined the zeroes of $h(\theta)$ and those of $z'(\theta)$. The latter define the location of singular points at which the

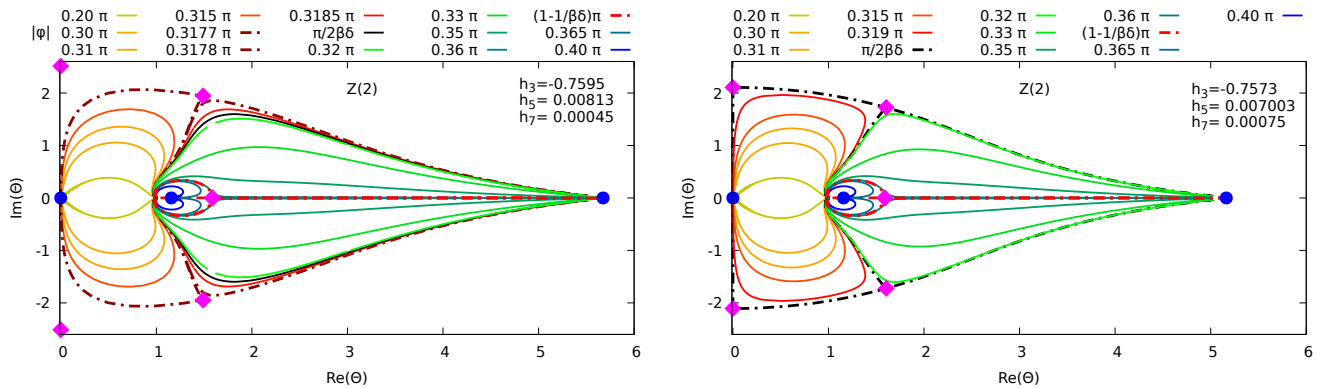


Figure 4. Contours in the complex θ -plane defined by values of z with constant phase ϕ , $z = |z| \exp(i\phi)$. Shown are results for the $Z(2)$ universality class using the function $h(\theta)$ with central values for (h_3, h_5, h_7) given in Eq. 41 (left) and tuned parameters that lead to a phase $\phi = \phi_{LY}$ (right). Dots show the location of zeroes of $h(\theta)$ and diamonds give locations of singularities in the susceptibility scaling functions $f'_G(z(\theta))$ and $f_\chi(z(\theta))$.

susceptibility scaling functions $f'_G(z)$ and $f_\chi(z)$ diverge, and the former gives points at which $z(\theta)$ diverges. In the limit $|z| \rightarrow \infty$ they are thus attractors for lines defined by $z = |z| \exp(i\phi)$.

Contrary to the situation met in the LPM approximation the complex z -plane is no longer mapped onto the entire complex θ half-plane with $\text{Re}(\theta) \geq 0$, but only to a finite region in that half-plane. The mapping $z \Leftrightarrow \theta$ is multi-valued. In Fig. 3 we show the contour plot of lines, $z = |z| \exp(i\phi)$ for constant phase ϕ obtained in the entire z plane for a particular set of parameters (h_3, h_5, h_7) . The part that provides a unique mapping is shown in Fig. 4. This unique mapping, $z \Leftrightarrow \theta$, is defined by lines $z = |z| \exp(i\phi)$, with $-\pi < \phi \leq \pi$ emerging from the point $\theta = 1$ at which $z = 0$ for all ϕ . These lines flow to $\theta = 0$ or one of the two real and positive zeroes, θ_0 and θ_1 , respectively.

As $z'(\theta)$ is even in θ one always finds sets of zeroes with positive and negative $\text{Re}(\theta)$. As a unique mapping of the complex z -plane to the θ -plane is already obtained by keeping only zeroes with $\text{Re}(\theta) \geq 0$, we will quote in the following only zeroes of $h(\theta)$ and $z'(\theta)$ with $\text{Re}(\theta) > 0$. We also note that due to the fact that $h(\theta)$ is an odd function in θ z -values obtained from θ and its negative counterpart are related to each other by

$$z(-\theta) = z(\theta) e^{-is/\beta\delta}, \quad s = \text{Arg}(\theta)/|\text{Arg}(\theta)|. \quad (44)$$

The region providing a unique mapping of the entire z -plane to the complex θ -plane is bounded by lines corresponding to $z(\theta) = |z| e^{\pm i r \phi_{LY}}$, which bifurcate at the complex points θ_{LY} and θ_{LY}^* , respectively. For $r = 1$ these points correspond to the Lee-Yang edge singularities, located in the complex z -plane at $z_{LY} = |z_{LY}| \exp(\pm i r \phi_{LY})$ (Fig. 4 (right)). However, as will be discussed below, due to truncation errors for the function $h(\theta)$ and statistical errors on the expansion parameters used in the definition of $h(\theta)$ one generally only finds $r \simeq 1$ (Fig. 4 (left)). At the bifurcation point $\pm\theta_{LY}$ the

	$ z_{Lan} $	$ z_{LY} $	$r \equiv \phi_{bi}/\phi_{LY}$
$c_2 = 0, c_4 = 0$	2.5429(8)	2.3177(40)	1
$c_2 \neq 0, c_4 = 0$	2.3693(93)	2.4398(63)	0.9855(23)
$c_2 \neq 0, c_4 \neq 0$	2.379(36)	2.418(55)	0.9935^{+45}_{-191}
Fig.4 (left)	2.3783	2.4177	0.9935
Fig.4 (right)	2.3827	2.4019	1

Table III. Absolute values of the Langer and Lee-Yang edge singularities obtained with different approximations for the function $h(\theta)$. The last column gives results for the phase ϕ_{bi} of the complex valued z at the bifurcation point. This should equal the Lee-Yang phase $\phi_{LY} = \pi/2\beta\delta$ with better controlled approximations for $h(\theta)$.

two emerging branches define branch cuts in the complex z -plane with phase $\phi_{bi} \equiv r\phi_{LY}$. The scaling function $f'_G(z(\theta))$ is discontinuous across this cut as well as across the Langer cut.

In Table III we give results for the Langer and Lee-Yang edge singularity obtained by (i) setting $c_2 = c_4 = 0$ (LPM approximation), (ii) setting only $c_4 = 0$, and (iii) keeping all three coefficients in the parameterization of $h(\theta)$ to be non-zero, respectively. As can be seen, the results for the absolute values of the edge singularities are fairly stable. The phase of the singularity, identified as the Lee-Yang edge singularity, agrees with $\phi_{LY} = \pi/2\beta\delta$ to better than 1%.

Already for $c_2 = c_4 = 0$ one obtains a pair of complex (purely imaginary) valued singular points, $\theta = \pm\theta_{LY}$, and a real, positive one at $\theta \equiv \theta_{Lan}$, which correspond to the location of the Lee-Yang and Langer edge singularities, respectively. For $c_2 \neq 0$ the singular points $\pm\theta_{LY}$ move into the complex plane.

With $c_4 \neq 0$ the location of the value of θ_{LY} and as such $z_{LY}(\theta_{LY})$ changes only slightly. In addition another pair of singularities shows up at $\theta_{LY,b}$. Given the currently large errors on c_4 the location of this second pair of zeroes of $z'(\theta)$ is not well controlled. For $c_4 > 0$ the

singularity is located on the real θ -axis. For $c_4 < 0$ it lies on the imaginary axis.

While variations of c_4 within its current errors thus influences the singular structure in the θ -plane, the location of Lee-Yang and Langer edge singularities at θ_{LY} gets modified only little. The main effect of a variation of c_4 within its errors is to increase the current error on the location of $z_{LY} \equiv z(\theta_{LY})$ and $z_{Lan} \equiv z(\theta_{Lan})$. We obtain

$$\begin{aligned} z_{LY} &= 2.418(55) e^{\pm i r \phi_{LY}}, \quad r = 0.9935_{-191}^{+45}, \\ z_{Lan} &= 2.379(36) e^{i \phi_{Lan}}. \end{aligned} \quad (45)$$

In Fig. 4 (left) we show the unique region for the mapping $z \leftrightarrow \theta$ and the location of zeroes and singular points in the θ -plane corresponding to the central values of (h_3, h_5, h_7) given in Eq. 41 that have been used to determine the location of the edge singularities given in Eq. 45. In the right hand figure we show results for a tuned set of parameters (h_3, h_5, h_7) , which leads to a bifurcation point having the correct phase of a Lee-Yang edge singularity. Branch cuts emerge from these edge singularities located on the dashed-dotted lines, which correspond to contours having the phase $\pm \phi_{LY}$ (black) and ϕ_{Lan} (red), respectively.

Starting from the edge singularities branch cuts emerge. These lead to discontinuities in the real and imaginary part of the scaling function $f_G(z)$. In Fig. 5 we show the gaps of $|f_G(z)|$ on the Langer and Lee-Yang branch cuts, respectively. As can be seen the magnitude of the discontinuity is quite different on these cuts. It is an order of magnitude larger on the Lee-Yang cut than on the Langer cut, which may be taken as an indication for the Langer edge singularity being an essential singularity [20] which leads to only a weak discontinuity across the cut. This, however, is not accessible with the truncated polynomial expansion used for $h(\theta)$. A more complicated form of $h(\theta)$ will be needed to reproduce the essential singularity at the Langer cut, as well as the universal form of the Lee-Yang edge singularity, which is expected to be described by a ϕ^3 -theory [12, 29, 30].

We conclude that results for the location of edge singularities in the $Z(2)$ universality class are quite stable and vary only little when adjusting the phase of $z(\theta_{LY})$. Even when moving from the LPM approximation to the currently known parameterization of the function $h(\theta)$ up to $O(\theta^7)$ the variation of $|z_{LY}|$ is only about 5%.

B. Lee-Yang edge singularities in the $O(N)$ universality classes

Aside from a 2-fold zero in the generalized LPM approximation for the function $h(\theta)$, which also is implemented in the general ansatz for $h(\theta)$ [37], the most important difference in corrections to the LPM approximation for $Z(2)$ and $O(N)$ universality classes, respectively, is due to the different sign of the coefficient c_2 in the leading order correction. As discussed above a consequence

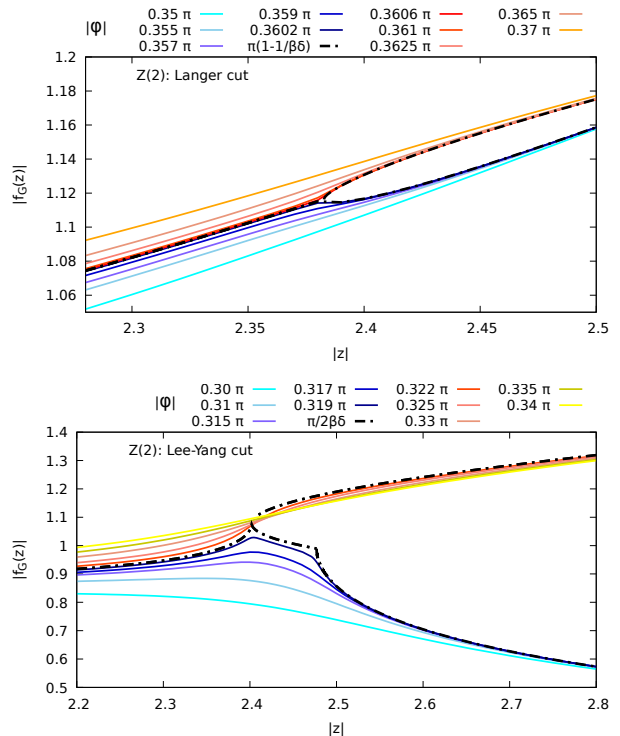


Figure 5. The absolute value of the $Z(2)$ scaling function $f_G(z)$ on the Langer (top) and Lee-Yang (bottom) cuts. Shown are results for the $Z(2)$ universality class using $h(\theta)$ with the tuned set of parameters (h_3, h_5, h_7) also used in Fig. 4 (right).

of this is that one always finds a pair of complex conjugate singularities in the susceptibility scaling functions located on the imaginary θ -axis at $\pm \theta_{LY,b}$, which corresponds to complex z -values with the Lee-Yang phase $\phi_{LY} = \pi/2\beta\delta$. Moreover, already for $c_2 = c_4 = 0$ one obtains a pair of singularities located at θ_{LY} in the complex θ -plane. As discussed in the previous subsection for the case of Lee-Yang singularities in the $Z(2)$ universality class, also in the $O(N)$ case the phase ϕ_{bi} at this singular point, $z(\theta_{LY})$, is not exactly at ϕ_{LY} . However, already for $c_2 \neq 0$ the phase ϕ_{bi} agrees with ϕ_{LY} within current statistical errors and this remains to be the case for $c_2 \neq 0$ and $c_4 \neq 0$. This behavior is found for the $O(2)$ as well as the $O(4)$ universality classes.

As has been done in the previous subsection for the $Z(2)$ universality class we also determined the absolute values of the Lee-Yang phase and the values for the phase $\phi_{bi} = r\phi_{LY}$ for three different cases: (i) $c_2 = c_4 = 0$, (ii) $c_2 = 0, c_4 \neq 0$, (iii) $c_2 \neq 0, c_4 \neq 0$. Our results are summarized in Table IV. In analogy to Fig. 4 we show in Fig. 6 contour plots in the $O(4)$ universality class. Fig. 6 (top, left) is for the set of central values for (θ_0, c_2, c_4) corresponding to $r = 1.023$ and the (bottom, left) figure corresponds to a parameter set with $\phi_{bi} = \phi_{LY}$, which lies inside the region defined by the current errors on (θ_0, c_2, c_4) .

	$O(2)$		$O(4)$	
	$ z_{LY} $	ϕ_{bi}/ϕ_{LY}	$ z_{LY} $	ϕ_{bi}/ϕ_{LY}
$c_2 = 0, c_4 = 0$	1.815(27)	0.868(7)	1.387(15)	0.789(9)
$c_2 \neq 0, c_4 = 0$	1.999(44)	1.037(33)	1.474(20)	1.027(34)
$c_2 \neq 0, c_4 \neq 0$	1.900(46)	1.024(30)	1.469(20)	1.023(34)
Fig. 6 (top)	–	–	1.469	1.023
Fig. 6 (bottom)	–	–	1.456	1

Table IV. Absolute values of the Lee-Yang edge singularities in the $O(2)$ and $O(4)$ universality classes obtained with different approximations for the function $h(\theta)$.

We note that the absolute value of the Lee-Yang edge singularity changes little when using only the LPM approximation for $h(\theta)$ or including the parameters c_2 and c_4 .

In the right hand column of Fig. 6 figure we show the absolute value of $f_G(z(\theta))$, evaluated on lines with constant phase $z = |z|e^{i\phi}$, $\phi \simeq \phi_{bi}$, versus $|z|$. The gap along the Lee-Yang branch cut clearly is visible. It is of similar magnitude as the discontinuity found in the $Z(2)$ universality class. We note that results obtained with the tuned parameter set (θ_0, c_2, c_4) and the central values determined for (θ_0, c_2, c_4) differ little in the location of the edge singularity as well as the size of the gap along the Lee-Yang branch cut.

V. CONCLUSIONS AND OUTLOOK

We give our final results for the location of Lee-Yang edge singularities of scaling functions in the $Z(2)$, $O(2)$ and $O(4)$ universality classes as well as the Langer edge singularity appearing in the scaling functions of the $Z(2)$ universality class in Table V. Here we have averaged over the results obtained when setting $c_4 = 0$ or using $c_4 \neq 0$ as discussed in the previous section. The difference between these two results is included as a systematic error that is added to the statistical error in quadrature. These results are compared with results obtained in FRG calculations [21, 22], which are given in the last row of Table V. As can be seen results in the $Z(2)$ and $O(2)$ universality classes, obtained from the Schofield parameterization of the magnetic equation of state and the FRG calculations, agree within the quoted errors while the result obtained in the $O(4)$ universality class differ by about 15%.

Also shown in the first row of Table V are results for the additional singularity at $z_{LY,b}$ that arises on the branch cuts. To what extent these singularities are artifacts of our current approximation for $h(\theta)$ remains to be analyzed by using higher order approximations for $h(\theta)$.

Also shown in Table V is the absolute value, $|z_{Lan}|$, for the location of the Langer edge singularity in. Although its central value is smaller than that for the location of the Lee-Yang edge singularity, it is consistent with $|z_{LY}|$ within errors.

We also have shown that the discontinuity of $f_G(z)$ on

	$Z(2): \mathcal{O}(\epsilon^2)$	$Z(2)$	$O(2)$	$O(4)$
$ z_{LY,b} $	–	–	2.281(72)	1.977(73)
$ z_{Lan} $	2.240	2.374(36)	–	–
$ z_{LY} $	2.307	2.429(56)	1.95(7)	1.47(3)
$ z_{LY} $ [FRG]		2.43(4)	2.04(8)	1.69(3)

Table V. Summary of results for absolute values of the location of the Lee-Yang edge singularities ($|z_{LY}|$ and the Langer edge singularity ($|z_{Lan}|$). In the first row we give the value for the location of a second singularity on the the Lee-Yang branch cut ($|z_{LY,b}|$ (see discussion in the text). The last row gives results from a FRG calculation [22].

the Langer branch cut is an order of magnitude smaller than the discontinuity occurring on the Lee-Yang branch cut. This may reflect the different critical behavior expected to control the divergence of susceptibilities at the edge singularities. This, however, cannot be resolved with the truncated series approximation used for the function $h(\theta)$ appearing in the Schofield parameterization of scaling functions. At present, the singular behavior at the edge singularities is identical at the Langer and Lee-Yang edge singularity as well as in all universality classes, due to the polynomial ansatz used for $h(\theta)$. This is because in all cases the singularity is determined by a zero of Eq. 15. With $h(\theta)$ being a polynomial in θ one can Taylor-expand in the vicinity of any of these zeroes, which generates a divergence at the Lee-Yang or Langer edge singularities being given by $1/(\theta - \theta_i)$, with $i = LY$ or Lan . It would be interesting to explore more refined analytic ansätze for $h(\theta)$ in the future.

All data from our calculations, presented in the figures of this paper, can be found in Ref.[49]

Acknowledgments. — This work was supported by The Deutsche Forschungsgemeinschaft (DFG, German Research Foundation) - Project number 315477589-TRR 211 and the PUNCH4NFDI consortium supported by the Deutsche Forschungsgemeinschaft (DFG, German Research Foundation) with project number 460248186 (PUNCH4NFDI).

Appendix A: $Z(2)$ parameters

We summarize here the determination of h_3 , h_5 and h_7 entering the parameterization of the function $h(\theta)$ in the $Z(2)$ universality class. We follow Ref. [35].

We use the critical exponents, also used in that calculation

$$\begin{aligned} \beta &= 0.3258(14), \\ \gamma &= 1.2396(13). \end{aligned} \quad (\text{A1})$$

In addition we also give results obtained by using recent, more accurate results for the critical exponents, obtained in Monte Carlo [44] and conformal bootstrap [45] calculations. Both approaches yield consistent results with

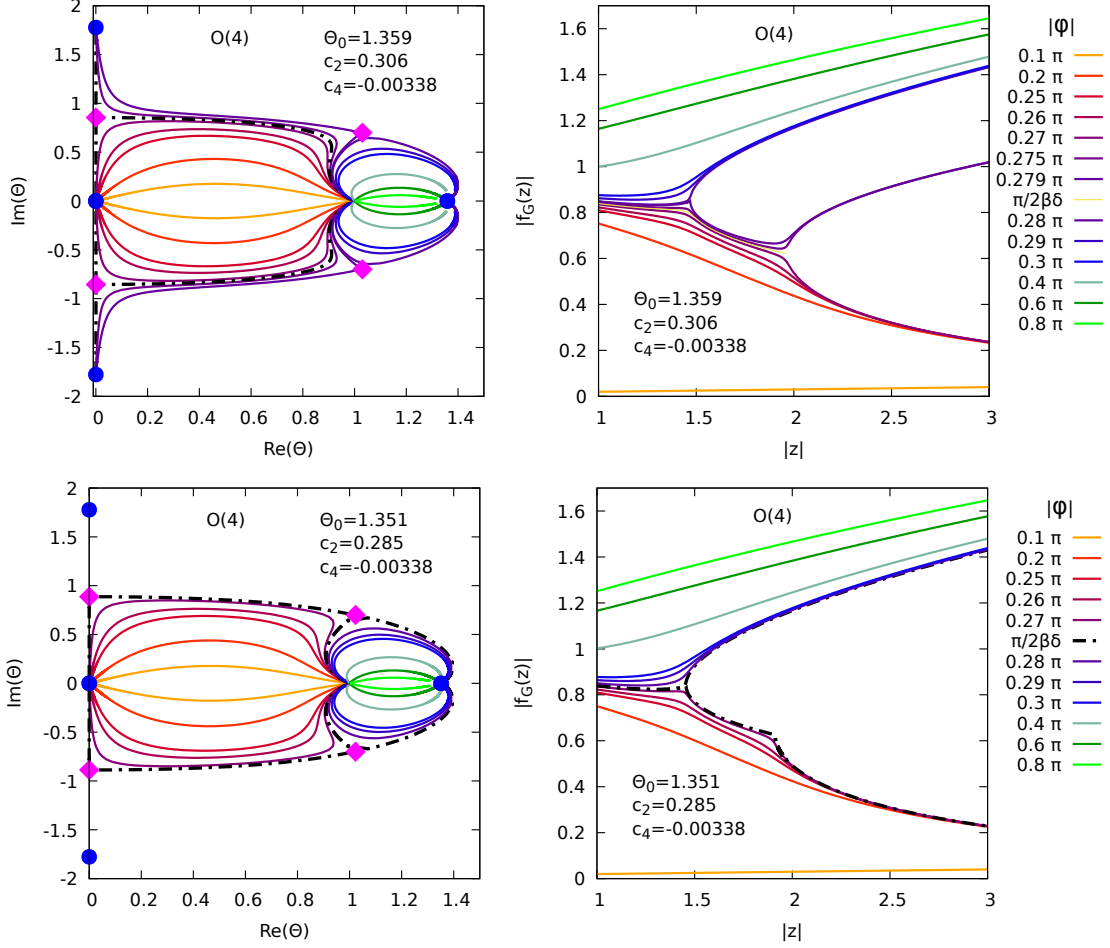


Figure 6. Contours in the complex θ -plane defined by values of z with constant phase ϕ , $z = |z| \exp(i\phi)$. Shown are results for the $O(4)$ universality class using $h(\theta)$ with the central values for (θ_0, c_2, c_4) given in Table II (top, left) and for a specific nearby choice of parameters (within the current errors) that correspond to $\phi = \phi_{LY}$ (bottom, left). The figures on the right show $|f_G(z)|$ for both cases. In the left hand figures dots show the location of zeroes of $h(\theta)$ and diamonds give locations of singularities in the susceptibility scaling functions $f'_G(z(\theta))$ and $f_\chi(z(\theta))$. Similar results can be obtained in the $O(2)$ universality class.

similarly small errors. The latter gives $\nu = 0.62999(5)$, $\eta = 0.03631(3)$. Using hyper-scaling relations we obtain

$$\begin{aligned} \beta &= 0.32643(7), \\ \gamma &= 1.23711(12). \end{aligned} \quad (\text{A2})$$

Using the hyper-scaling relation, $\delta = (\gamma + \beta)/\beta$, we obtain $\delta = 4.8048(20)$ using Eq. A1 and $\delta = 4.7898(12)$ using Eq. A2.

We compare results for (h_3, h_5, h_7) obtained with these updated critical exponents to those obtained in Ref. [35] in Table VI.

The coefficients (h_3, h_5, h_7) have been determined in [35] using resummed results of a $3-d$ perturbative expansion of the function $F(z)$, which is defined as derivative of the free energy with respect to a variable \tilde{z} ,

$$F(\tilde{z}) = \tilde{z} + \frac{1}{6}\tilde{z}^3 + F_5\tilde{z}^5 + F_7\tilde{z}^7, \quad (\text{A3})$$

with

$$F_5 = 0.01711(7), \quad F_7 = 0.00049(5). \quad (\text{A4})$$

The expansion parameter \tilde{z} is related to the variable θ , used in the Schofield parameterization, through,

$$\tilde{z} = \rho\theta/(1 - \theta^2)^\beta. \quad (\text{A5})$$

In [35] the scale parameter $\rho^2 = 2.8656$ is used. We assign an error of 10^{-2} to it⁵.

The function $F(\tilde{z})$ is related to $h(\theta)$ through

$$h(\theta) = \rho^{-1}(1 - \theta^2)^{\beta\delta}F(\tilde{z}(\theta)). \quad (\text{A6})$$

⁵ No error on ρ^2 has been quoted in [35]. The error assigned by us, however, reproduces the error on h_3 and h_5 given in that reference.

h_3	h_5	h_7
-0.7620(30)	0.00818 (92)	0.00024 (128)
-0.7595(18)	0.00813(68)	0.00045 (127)

Table VI. Expansion coefficients of $h(\theta)$. The first row gives results obtained by using the critical exponents determined in [35] and the last row uses the bootstrap results from [45].

Expanding the right hand side of this equation in terms of θ and using

$$h(\theta) = \theta(1 + h_3\theta^2 + h_5\theta^4 + h_7\theta^6 + \dots), \quad (\text{A7})$$

one arrives at relations for (h_3, h_5, h_7) in terms of the expansion coefficients (F_3, F_5, F_7) ,

$$h_3 = \frac{1}{6}\rho^2 - \gamma, \quad (\text{A8})$$

$$h_5 = \frac{1}{2}\gamma(\gamma - 1) + \frac{1}{6}(2\beta - \gamma)\rho^2 + F_5\rho^4, \quad (\text{A9})$$

$$h_7 = -\frac{1}{6}\gamma(\gamma - 1)(\gamma - 2) + \frac{1}{12}(2\beta - \gamma)(2\beta - \gamma + 1)\rho^2 + (4\beta - \gamma)F_5\rho^4 + F_7\rho^6. \quad (\text{A10})$$

Note that the sign of the first term in the relation for h_7 is opposite to that quoted in [35]. Using these relations we reproduce the expansion coefficients h_3, h_5 , given in [35] and obtain results for h_7 consistent with statements

made in the [35] about the magnitude of h_7 . These numbers are given in Table VI. We also reproduce the errors quoted for h_3 and h_5 in [35].

Using results for (h_3, h_5, h_7) we can calculate the coefficients (θ_0, c_2, c_4) appearing in the parameterization of $h(\theta)$ given in Eq. 39. For c_2 and c_4 one obtains,

$$c_2 = -(h_5 + h_7\theta_0^2)\theta_0^2, \quad (\text{A11})$$

$$c_4 = -h_7\theta_0^2, \quad (\text{A12})$$

and θ_0 is obtained as the real, positive zero of $h(\theta)$, defined in Eq. 40, which is closest to $\theta = 1$.

Using the parameters given in the last row of Table VI we obtain for the first zero of $h(\theta)$,

$$\theta_0 = 1.1564(39), \quad (\text{A13})$$

and the absolute value of the Langer edge singularity is,

$$|z_{Lan}| = 2.379(36). \quad (\text{A14})$$

We furthermore find two singular points with a phase that is close to or identical to that expected for the Lee-Yang cut, $\phi_{LY} = \pi/2\beta\delta$. The edge singularity has an absolute value,

$$|z_{LY}| = 2.418_{-0.068}^{+0.043}, \quad (\text{A15})$$

with a phase that is consistent with ϕ_{LY} . For the second singular point the absolute value is,

$$|z_{LY,b}| = 2.452_{-0.012}^{+0.034}, \quad (\text{A16})$$

and the phase equals ϕ_{LY} .

-
- [1] F. Gross *et al.*, 50 Years of Quantum Chromodynamics, (2022), arXiv:2212.11107 [hep-ph].
- [2] O. Philipsen, Lattice Constraints on the QCD Chiral Phase Transition at Finite Temperature and Baryon Density, *Symmetry* **13**, 2079 (2021), arXiv:2111.03590 [hep-lat].
- [3] J. N. Guenther, An overview of the QCD phase diagram at finite T and μ , *PoS LATTICE2021*, 013 (2022), arXiv:2201.02072 [hep-lat].
- [4] M. D'Elia and M.-P. Lombardo, Finite density QCD via imaginary chemical potential, *Phys. Rev. D* **67**, 014505 (2003), arXiv:hep-lat/0209146.
- [5] P. de Forcrand and O. Philipsen, The QCD phase diagram for small densities from imaginary chemical potential, *Nucl. Phys. B* **642**, 290 (2002), arXiv:hep-lat/0205016.
- [6] R. V. Gavai and S. Gupta, Quark number susceptibilities, strangeness and dynamical confinement, *Phys. Rev. D* **64**, 074506 (2001), arXiv:hep-lat/0103013.
- [7] C. R. Allton, S. Ejiri, S. J. Hands, O. Kaczmarek, F. Karsch, E. Laermann, C. Schmidt, and L. Scorzato, The QCD thermal phase transition in the presence of a small chemical potential, *Phys. Rev. D* **66**, 074507 (2002), arXiv:hep-lat/0204010.
- [8] D. Bollweg, J. Goswami, O. Kaczmarek, F. Karsch, S. Mukherjee, P. Petreczky, C. Schmidt, and P. Scior (HotQCD), Taylor expansions and Padé approximants for cumulants of conserved charge fluctuations at nonvanishing chemical potentials, *Phys. Rev. D* **105**, 074511 (2022), arXiv:2202.09184 [hep-lat].
- [9] C. N. Yang and T. D. Lee, Statistical theory of equations of state and phase transitions. i. theory of condensation, *Phys. Rev.* **87**, 404 (1952).
- [10] T. D. Lee and C. N. Yang, Statistical theory of equations of state and phase transitions. ii. lattice gas and ising model, *Phys. Rev.* **87**, 410 (1952).
- [11] X. An, D. Mesterházy, and M. A. Stephanov, Functional renormalization group approach to the Yang-Lee edge singularity, *JHEP* **07**, 041, arXiv:1605.06039 [hep-th].
- [12] X. An, D. Mesterházy, and M. A. Stephanov, On spinodal points and Lee-Yang edge singularities, *J. Stat. Mech.* **1803**, 033207 (2018), arXiv:1707.06447 [hep-th].
- [13] S. Mukherjee and V. Skokov, Universality driven analytic structure of the QCD crossover: radius of convergence in the baryon chemical potential, *Phys. Rev. D* **103**, L071501 (2021), arXiv:1909.04639 [hep-ph].

- [14] S. Mukherjee, F. Rennecke, and V. V. Skokov, Analytical structure of the equation of state at finite density: Resummation versus expansion in a low energy model, *Phys. Rev. D* **105**, 014026 (2022), arXiv:2110.02241 [hep-ph].
- [15] G. Basar, Universality, Lee-Yang Singularities, and Series Expansions, *Phys. Rev. Lett.* **127**, 171603 (2021), arXiv:2105.08080 [hep-th].
- [16] G. Basar, G. V. Dunne, and Z. Yin, Uniformizing Lee-Yang singularities, *Phys. Rev. D* **105**, 105002 (2022), arXiv:2112.14269 [hep-th].
- [17] P. Dimopoulos, L. Dini, F. Di Renzo, J. Goswami, G. Nicotra, C. Schmidt, S. Singh, K. Zambello, and F. Ziesché, Contribution to understanding the phase structure of strong interaction matter: Lee-Yang edge singularities from lattice QCD, *Phys. Rev. D* **105**, 034513 (2022), arXiv:2110.15933 [hep-lat].
- [18] C. Schmidt, D. A. Clarke, G. Nicotra, F. Di Renzo, P. Dimopoulos, S. Singh, J. Goswami, and K. Zambello, Detecting Critical Points from the Lee-Yang Edge Singularities in Lattice QCD, *Acta Phys. Polon. Supp.* **16**, 1 (2023), arXiv:2209.04345 [hep-lat].
- [19] D. A. Clarke, K. Zambello, P. Dimopoulos, F. Di Renzo, J. Goswami, G. Nicotra, C. Schmidt, and S. Singh, Determination of Lee-Yang edge singularities in QCD by rational approximations, *PoS LATTICE2022*, 164 (2023), arXiv:2301.03952 [hep-lat].
- [20] J. S. Langer, Theory of the condensation point, *Annals Phys.* **41**, 108 (1967).
- [21] A. Connelly, G. Johnson, F. Rennecke, and V. Skokov, Universal Location of the Yang-Lee Edge Singularity in $O(N)$ Theories, *Phys. Rev. Lett.* **125**, 191602 (2020), arXiv:2006.12541 [cond-mat.stat-mech].
- [22] G. Johnson, F. Rennecke, and V. V. Skokov, Universal location of Yang-Lee edge singularity in classic $O(N)$ universality classes, *Phys. Rev. D* **107**, 116013 (2023), arXiv:2211.00710 [hep-ph].
- [23] P. Schofield, Parametric representation of the equation of state near a critical point, *Phys. Rev. Lett.* **22**, 606 (1969).
- [24] P. Schofield, J. D. Litster, and J. T. Ho, Correlation between critical coefficients and critical exponents, *Phys. Rev. Lett.* **23**, 1098 (1969).
- [25] B. Widom, Equation of State in the Neighborhood of the Critical Point, *J. Chem. Phys.* **43**, 3898 (1965).
- [26] R. B. Griffiths, Thermodynamic functions for fluids and ferromagnets near the critical point, *Phys. Rev.* **158**, 176 (1967).
- [27] J. Engels and T. Mendes, Goldstone mode effects and scaling function for the three-dimensional $O(4)$ model, *Nucl. Phys. B* **572**, 289 (2000), arXiv:hep-lat/9911028.
- [28] F. Karsch, M. Neumann, and M. Sarkar, Scaling functions of the three-dimensional $Z(2)$, $O(2)$, and $O(4)$ models and their finite-size dependence in an external field, *Phys. Rev. D* **108**, 014505 (2023), arXiv:2304.01710 [hep-lat].
- [29] M. E. Fisher, Yang-lee edge singularity and ϕ^3 field theory, *Phys. Rev. Lett.* **40**, 1610 (1978).
- [30] P. Fonseca and A. Zamolodchikov, Ising field theory in a magnetic field: Analytic properties of the free energy, (2001), arXiv:hep-th/0112167.
- [31] M. Hasenbusch, A Monte Carlo study of leading order scaling corrections of ϕ^4 theory on a three-dimensional lattice, *J. Phys. A* **32**, 4851 (1999), arXiv:hep-lat/9902026.
- [32] J. Engels, S. Holtmann, T. Mendes, and T. Schulze, Equation of state and Goldstone mode effects of the three-dimensional $O(2)$ model, *Phys. Lett. B* **492**, 219 (2000), arXiv:hep-lat/0006023.
- [33] J. Engels, L. Fromme, and M. Seniuch, Numerical equation of state from an improved three-dimensional Ising model, *Nucl. Phys. B* **655**, 277 (2003), arXiv:cond-mat/0209492.
- [34] R. Guida and J. Zinn-Justin, 3-D Ising model: The Scaling equation of state, *Nucl. Phys. B* **489**, 626 (1997), arXiv:hep-th/9610223.
- [35] R. Guida and J. Zinn-Justin, Critical exponents of the N vector model, *J. Phys. A* **31**, 8103 (1998), arXiv:cond-mat/9803240.
- [36] M. Campostrini, M. Hasenbusch, A. Pelissetto, P. Rossi, and E. Vicari, Critical behavior of the three-dimensional xy universality class, *Phys. Rev. B* **63**, 214503 (2001), arXiv:cond-mat/0010360.
- [37] M. Campostrini, A. Pelissetto, P. Rossi, and E. Vicari, The Critical equation of state of three-dimensional X Y systems, *Phys. Rev. B* **62**, 5843 (2000), arXiv:cond-mat/0001440.
- [38] M. Campostrini, M. Hasenbusch, A. Pelissetto, P. Rossi, and E. Vicari, Critical exponents and equation of state of the three-dimensional Heisenberg universality class, *Phys. Rev. B* **65**, 144520 (2002), arXiv:cond-mat/0110336.
- [39] J. Engels and F. Karsch, The scaling functions of the free energy density and its derivatives for the 3d $O(4)$ model, *Phys. Rev. D* **85**, 094506 (2012), arXiv:1105.0584 [hep-lat].
- [40] D. S. Gaunt and C. Domb, Equation of state of the ising model near the critical point, *Journal of Physics C: Solid State Physics* **3**, 1442 (1970).
- [41] E. Brézin, D. J. Wallace, and K. G. Wilson, Feynman-graph expansion for the equation of state near the critical point (ising-like case), *Phys. Rev. Lett.* **29**, 591 (1972).
- [42] D. J. Wallace and R. K. P. Zia, Parametric models and the Ising equation of state at order ϵ^{**3} , *J. Phys. A* **7**, 3480 (1974).
- [43] G. A. Almasi, W. Tarnowski, B. Friman, and K. Redlich, Scaling violation and the magnetic equation of state in chiral models, *Phys. Rev. D* **95**, 014007 (2017), arXiv:1605.05423 [hep-ph].
- [44] M. Hasenbusch, Finite size scaling study of lattice models in the three-dimensional Ising universality class, *Phys. Rev. B* **82**, 174433 (2010), arXiv:1004.4486 [cond-mat.stat-mech].
- [45] S. El-Showk, M. F. Paulos, D. Poland, S. Rychkov, D. Simmons-Duffin, and A. Vichi, Solving the 3d Ising Model with the Conformal Bootstrap II. c-Minimization and Precise Critical Exponents, *J. Stat. Phys.* **157**, 869 (2014), arXiv:1403.4545 [hep-th].
- [46] M. Hasenbusch, Monte Carlo study of an improved clock model in three dimensions, *Phys. Rev. B* **100**, 224517 (2019), arXiv:1910.05916 [cond-mat.stat-mech].
- [47] J. Engels, L. Fromme, and M. Seniuch, Correlation lengths and scaling functions in the three-dimensional $O(4)$ model, *Nucl. Phys. B* **675**, 533 (2003), arXiv:hep-lat/0307032.
- [48] J. Zinn-Justin, Precise determination of critical exponents and equation of state by field theory methods, *Phys. Rept.* **344**, 159 (2001), arXiv:hep-th/0002136.
- [49] F. Karsch, C. Schmidt, and S. Singh, Dataset for

"lee-yang and langer edge singularities from analytic

continuation of scaling functions", Bielefeld University
10.4119/unibi/2985954 (2024).